Carbohydrate-based polyamides and polyesters: an overview illustrated with two selected examples

Sebastián Muñoz-Guerra

High Performance Polymers 2012 24: 9 originally published online 7 March 2012

DOI: 10.1177/0954008311429502

Article

High Performance Polymers

High Performance Polymers
24(1) 9–23

DOI: 10.1177/0954008311429502
hip.sagepub.com

Carbohydrate-based polyamides and polyesters: an overview illustrated with two selected examples

Sebastián Muñoz-Guerra

Abstract

An overview on the synthesis, structure and properties of polyamides and aromatic copolyesters produced by using monomers derived from carbohydrates is provided. Two examples are selected for illustration: (a) aliphatic polyamides prepared from aldaric acids and (b) aromatic copolyesters containing alditols units. Polycondensation in solution of *n*-alkanediamines (*n* taking even values from 6 to 12) with activated pentaric (L-*arabino* and *xylo*) and hexaric (*galacto* and D-*manno*) acids bearing the secondary hydroxyl groups protected as methyl ether, afforded linear polyaldaramides PA-*n*Su with M_w oscillating between 25 000 and 150 000 g mol^{-1}. They are stable above 300°C and are semicrystalline even so only PA-*n*Mn are stereoregular. Melting temperatures of PA-*n*Su range between 140 and 230°C and most of them are able to crystallize from the melt at a rate that increases with the length of the polymethylene segment. Both melting and glass transition temperatures decrease with the content in sugar units. Spherulitic films, oriented fibers and lamellar single crystals could be obtained from PA-*n*Su. All these polyamides seem to adopt a common crystal structure made of hydrogen-bonded sheets with the sugar residue skewed to attain an efficient side-by-side packing of the polymer chains. Aromatic homopolyesters and copolyesters derived from terephthalic acid and mixtures of butylene glycol and *O*-methylated alditols were prepared by polycondensation in the melt with M_w in the 20 000–50 000 g mol^{-1} range and a random microstructure. The thermal properties of PBT containing alditols units are very depending on the sugar constitution and copolyester composition. In general they are thermally stable above 300°C and display crystallinity for contents in alditols up to 30%. Melting temperatures decrease with the content in alditols whereas an opposite trend is observed for glass transition temperatures. The crystalline structure of PBT is preserved in the crystalline copolyesters whereas a different crystal lattice is adopted by homopolyesters entirely made of alditol units. In general, polyamides and polyesters containing sugar derived units are widely soluble in organic solvents, markedly hydrophilic and more susceptible to hydrolysis than their parent polymers.

Keywords

sugar-based polyamides, sugar-based aromatic copolyesters, carbohydrate-based polymers

Introduction

Carbohydrates are widely spread naturally-occurring compounds offering outstanding advantages for the preparation of bio-based polymers.[1] Carbohydrates are fully renewable, easily accessible and widely diverse. The hydroxyl- and carboxylic-rich functionality of these compounds makes them particularly appropriate for polycondensation in spite of the fact that certain chemical handling for group protection and activation will be required if linear polymers are searched (Scheme 1). Carbohydrate-based polycondensates may be provided with a great variety of chemical structures and unusual properties; they typically display enhanced hydrophilicity, and they are more prone to be non-toxic and biodegradable than petrochemical-based polycondensates, offering therefore a wide possibility of applications in food packaging and medical devices.[2,3]

Our interests are mainly addressed to the synthesis of linear polycondensates made from difunctional monomers derived from carbohydrates. Readily available monosaccharides either produced by degrading polysaccharides or

Department of Chemical Engineering, ETSEIB, Universitat Politècnica de Catalunya, Barcelona, Spain

Corresponding Author:
Sebastián Muñoz-Guerra, Department of Chemical Engineering, ETSEIB Diagonal 647, Universitat Politècnica de Catalunya, Barcelona 08028, Spain
Email: sebastian.munoz@upc.edu

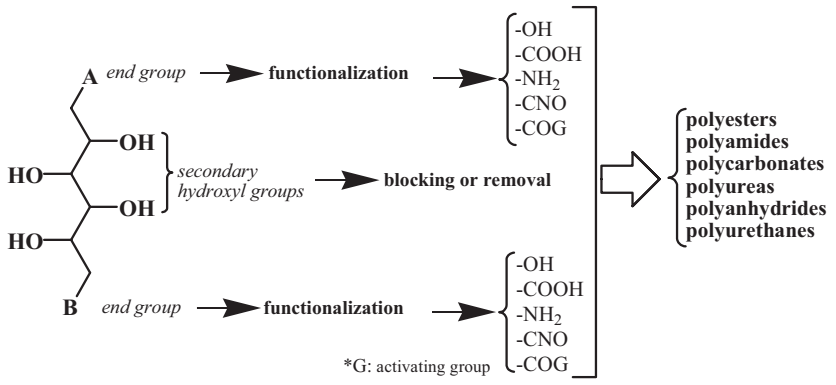

Scheme 1. Linear polycondensates from carbohydrates.

simply recovered from natural resources, are conveniently modified to afford aldaric acids, alditols and diaminoalditols suitable for polycondensation. A variety of polyamides,[4–12] polyesters,[13–17] and polyesteramides[18–25] as well as other polycondensates[26] derived from tetroses, pentoses and hexoses have been thus obtained and characterized, their structure examined, and some of their more relevant properties comparatively evaluated. We have been dedicated to the research of carbohydrate-based linear polycondensates for more than two decades so a pretty wide number of systems have been studied so far. In this presentation I wish to give an overview of our work illustrated with two representative examples: *polyaldaramides,* which are the linear polyamides made from aldaric acids and aliphatic diamines,[27,28], and *aromatic copolyesters* which are obtained by polycondensation of mixtures of alditols and alkanediols with dimethyl terephthalate (DMT)[29] (Scheme 2).

The chemistry involved in the preparation of monomers is relatively simple. Precursors, which can be aldoses, aldonic acids, lactones, etc., are properly functionalized and conveniently protected (Scheme 3). Depending on the precursor and the needed function, functionalization may involve oxidation of carbonyl or/and hydroxymethyl end groups to form the aldaric acid, or reduction of carbonyl or/and carboxylic groups to generate the alditol. Protection of secondary hydroxyl groups is necessary to avoid branching or cross-linking reactions. *O*-methylation was the protecting method mostly used because it does not affect the sugar configuration and provides an ether group that is stable during the polycondensation reaction as well as during polymer handling. Lastly, activation of the carboxylic group may be also advisable in order to improve polycondensation speed and yield.

An important issue of these syntheses is carbohydrate configuration because it will determine the microstructure of the resulting polycondensates and their properties to a large extent. In Scheme 4, the sugar configurations used in the two systems described in this paper are depicted. The selection comprises configurations with three and four asymmetric carbon atoms and with different symmetry properties. Only the *manno* configuration has a two-fold

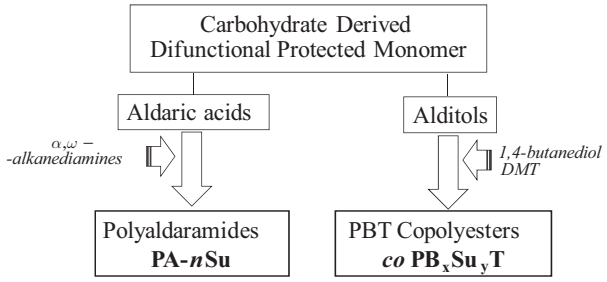

Scheme 2. Polyaldaramides and copolyesters from carbohydrates described in this paper.

symmetry axis and therefore only the polycondensates made from this configuration will be stereoregular. It should be stressed that all the other configurations will produce non-stereoregular polymers because two orientations are feasible for the incorporation of the sugar in the growing polymer chain. With regards to optical activity, *xylo* and *galacto* configurations contain an inversion center and are therefore non-chiral, and their corresponding polycondensates will not exhibit optical rotation. The *arabino* configuration lacks any symmetry element other than the identity, and its polycondensates will be therefore non-stereoregular but optically active.

Experimental section

Materials

Chemicals were all used as purchased from Aldrich Chemical Co. Solvents were dried and purified, when necessary, by appropriate standard procedures. The synthesis of alditols and pentachlorophenyl esters of aldaric acids protected as methyl ethers has been previously described in detailed elsewhere.[30,31]

Synthesis

Polyamides PA-nAr and PA-nXy.

Method A: To a stirred solution of the activated ester of the aldaric acid (Ar or Xy, 1 mmol) in dry chloroform

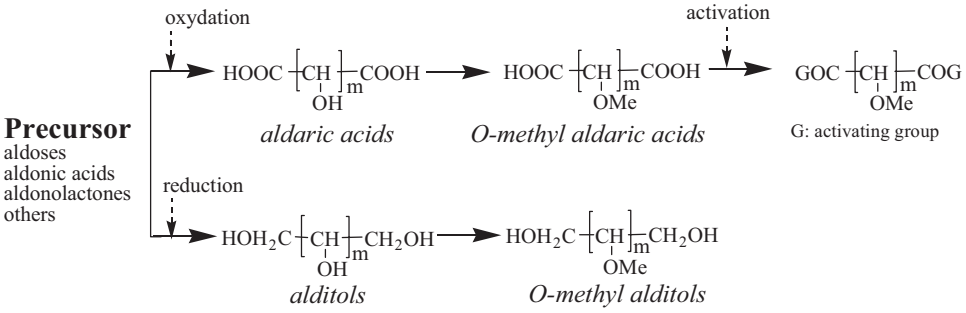

Scheme 3. Protection and activation of aldaric acids and alditols.

(1.5 mL), at 0°C under argon, was added dropwise the corresponding freshly prepared *N, N′*-trimethylsilylalkanediamine (1 mmol). The mixture was allowed to reach room temperature and left to proceed for 3 days. Then the reaction mixture was diluted with chloroform, and the solution heated at 60°C for 2 h. Method B: To a stirred suspension of the activated ester of the aldaric acid (Ar or Xy, 1 mmol) and the corresponding diamine (1 mmol) in dry *N*-methyl-2-pyrrolidinone (8 mL) was added *N*-ethyl-*N,N*-diisopropylamine (1.2 mL), and the mixture was stirred at 45°C under argon for at least a week. In both methods, the resulting polyamide was precipitated by pouring the reaction mixture onto diethyl ether and the precipitate was filtered and washed successively with diethyl ether, acetone, ethanol, and diethyl ether. The solid was finally dried under vacuum at 40°C

Polyamides PA-nGa and PA-nMn. For the case of PA-*n*Ga, dry *N*-methylpyrrolidinone (2 mL) was added to a mixture of galactaric acid activated as pentachloropenyl ester (0.25 mmol) and the corresponding diamine (0.25 mmol) placed under N_2, and the mixture was stirred at 45°C for 7 days. For the case of PA-*n*Mn, dry chloroform (4 mL) was added to a mixture of the L-mannaric acid activated as pentachlorophenyl ester (0.5 mmol) and the corresponding diamine (0.5 mmol) placed under N_2, and the mixture was stirred at room temperature for 7 days and then heated at 60°C for 1 h. In both cases, the reaction mixture was diluted with dichloromethane (5 mL) and added dropwise to diethyl ether (200 mL) with stirring. The white precipitate was filtered, washed with diethyl ether, and dried under diminished pressure.

Copolyesters coPB$_x$Ar$_y$T and coPB$_x$Xy$_y$T. A magnetically stirred mixture of 2,3,4-tri-*O*-methyl-L-arabinitol or 2,3,4-tri-*O*-methyl-xylitol, 1,4-butanediol, and dimethyl terephthalate, in a molar ratio of the two diols to DMT of 2.2/1 was slowly heated to 180°C under an argon atmosphere. After standing 1.5 h at this temperature, 0.6 mmol of titanium tetrabutoxide was added, and the mixture was heated first for 4 h at 195°C, and finally for 3 h at 200°C under vacuum (0.5–1 mm-Hg). The same procedure was used for the synthesis of homopolyesters made from alditols, and for the synthesis of PBT, the second stage was

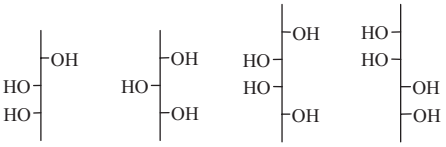

Configuration	L-*arabino*	*xylo*	*galacto*	D-*manno*
Number of C *	3	3	4	4
Symmetry	1	*i*	*i*	C_2
Stereoregularity	-	-	-	+
Optical activity	+	-	-	+

Scheme 4. Sugar configurations: symmetry and properties.

carried out at 250°C. After cooling the reaction mixture to room temperature, the resulting slightly colored solid was dissolved in the minimum amount of chloroform or a trifluoroacetic acid–chloroform mixture, and the solution was poured dropwise into diethyl ether. The precipitated white solid was purified by repeating the solution-precipitation procedure several times.

Methods

Optical rotations were measured in a Perkin-Elmer 341 polarimeter at 20 ± 5°C in an 1 cm-cell. IR spectra (films or KBr disks) were recorded with a JASCO FT/IR-410 spectrometer. Gel permeation chromatography (GPC) analyses were carried out on a Waters GPC system equipped with a refractive index detector using chloroform as the mobile phase at a flow rate of 1 mL min^{-1}. Molecular weights were calculated against monodisperse polystyrene standards using the Maxima 820 software. Intrinsic viscosity measurements were carried out in dichloroacetic acid with a Cannon-Ubbelohde 100/L30 semimicroviscometer at 25.0 ± 0.1°C. NMR spectra of polyamides were registered at 200 MHz for ^{1}H and 50 MHz on a Bruker 200 AC-P. For polyesters ^{1}H- and ^{13}C-NMR spectra were recorded on a Bruker AMX-300 spectrometer at 25.0°C operating at 300.1 and 75.5 MHz, respectively. Polyesters and copolyesters were dissolved in a mixture of deuterated chloroform and trifluoroacetic acid (9: 1), and spectra were internally referenced to tetramethylsilane (TMS). Here 10

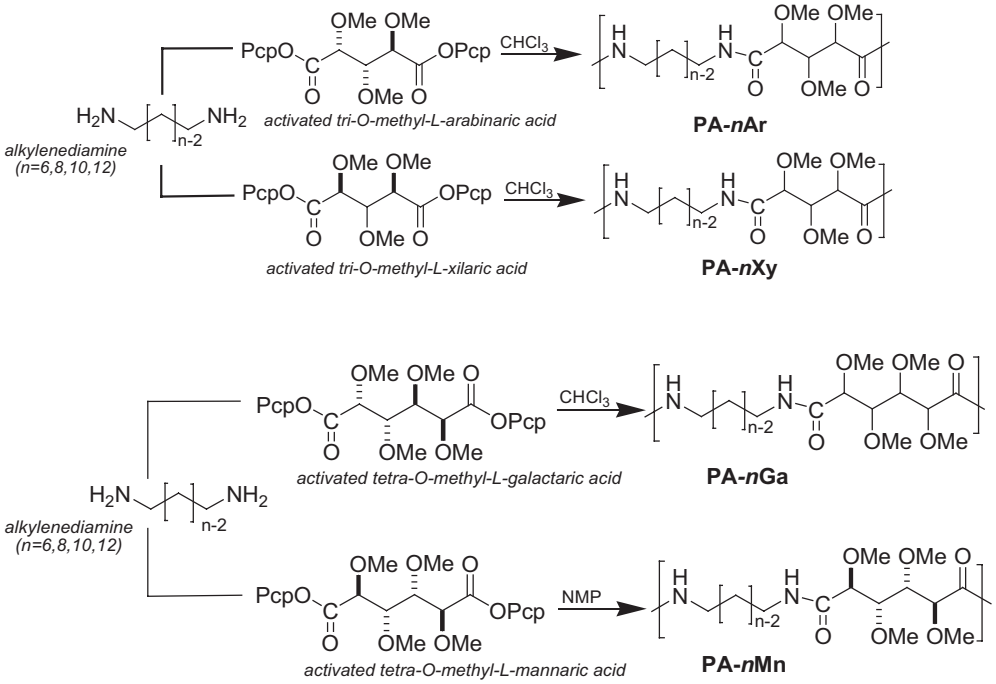

Scheme 5. Synthesis of polyaldaramides.

and 50 mg of sample dissolved in 1 mL of deuterated solvent were used for ^{1}H- and ^{13}C-NMR, respectively. Sixty-four scans were acquired for ^{1}H and 1000–10 000 for ^{13}C with 32 000 and 64 000 data points and relaxation delays of 1 and 2 s, respectively.

The thermal behavior of the polyesters was examined by differential scanning calorimetry (DSC) using a Perkin-Elmer DSC Pyris 1 calibrated with indium. DSC data were obtained from samples of 4–6 mg at heating/cooling rates of 10 or 20°C min^{-1} under nitrogen circulation. The glass-transition temperatures were determined at a heating rate of 20°C min^{-1} from rapidly melt-quenched polymer samples. Isothermal crystallization studies were made from samples heated to 250°C, maintained at this temperature for 5 min, and then quickly cooled to the crystallization temperature T_c. The heat flow evolving during the isothermal crystallization was recorded as a function of time. Thermogravimetric analysis (TGA) was carried out with a Perkin-Elmer TGA-6 thermobalance at a heating rate of 10°C min^{-1} under a nitrogen atmosphere.

Electron microscopy observations were carried out on a Phillips-Tecnai instrument operating at 80 and 100 kV for bright field (digital camera attached) and electron diffraction modes, respectively. Lamellar crystals were prepared by crystallization of the polyamides from diluted solutions (0.1% w/v) in glycerine at 130°C. Electron diffraction patterns were recorded in the selected area mode from non-shadowed samples, and they were internally calibrated with gold (d_{111}: 0.235 nm). Powder X-ray diffraction patterns were recorded on flat photographic films with a modified Statton camera using nickel-filtered Cu Kα radiation with wavelength 0.1542 nm, and they were calibrated with molybdenum sulphide ($d_{002} = 6.147$ Å). Optical microscope observations were made with an Olympus polarizing microscope equipped with a Linkam thermal stage. Hydrolysis experiments were carried out on disks prepared by casting at room temperature from a 10% (w/v) solution in chloroform. Disks were separately immersed in both acidic (pH 2.0 or 4.0) and basic (pH 10.6) 0.1 mol L^{-1} buffer solutions at 80°C. After immersion for a fixed period of time, the remaining solid was recovered, rinsed with water, and dried to constant weight under vacuum. The evolution of degradation was followed by GPC and NMR.

Results and discussion

Polyaldaramides

Synthesis and characterization. The method used for the synthesis of polyamides made from aldaric acids is presented in Scheme 5. The L-arabinaric and xylaric acids activated as pentachlorophenol esters, and conveniently protected as methyl ethers, were made to react with alkylenediamines in chloroform solution at slightly above room temperature to render the corresponding polyaldaramides PA-*n*Ar and PA-*n*Xy, respectively, with satisfactory molecular weights and polydispersities. Occasionally some diamines were converted in their corresponding trimethylsilane derivatives to speed the polycondensation reaction

Table 1. Synthesis results of polyaldaramides.

PA-nAr	Solvent	Yield (%)	M_w (g mol^{-1})	PD	$[\alpha]_D$ (deg)
PA-6Ar	$CHCl_3$	70	86 600	1.60	n.d.
PA-8Ar	$CHCl_3$	50	53 400	1.36	n.d.
PA-10Ar	$CHCl_3$	90	136 000	1.90	n.d.
PA-12Ar	$CHCl_3$	90	51 700	1.46	n.d.
PA-6Xy	$CHCl_3$	80	62 300	1.49	n.o.
PA-8Xy	$CHCl_3$	80	78 400	1.59	n.o.
PA-12Xy	$CHCl_3$	60	158 000	1.48	n.o.
PA-6Ga	NMP	85	25 100	1.60	n.o.
PA-8Ga	NMP	95	55 300	1.45	n.o.
PA-10Ga	NMP	95	72 100	1.36	n.o.
PA-12Ga	NMP	85	108 000	1.42	n.o.
PA-6Mn	$CHCl_3$	80	42 300	1.37	+48
PA-8Mn	$CHCl_3$	80	78 400	1.37	+40
PA-10Mn	$CHCl_3$	80	71 000	1.55	+56
PA-12Mn	$CHCl_3$	75	158 000	1.27	+32

n.d., not determined; n.o., not observed.

and increase yields. Exactly the same synthetic procedure was applied to galactaric and D-mannaric acids with similar results with the exception that *N*-methylpyrrolidone (NMP) had to be used as solvent in the polycondensation of D-mannaric acid due to solubility requirements. All the obtained polyamides were soluble in chloroform and they were isolated by precipitation with ether and purified by reprecipitation in chloroform-ether.

The results attained in these syntheses are summarized in Table 1. Yields were acceptably high in general and molecular weights exceeded the minimum values usually required for conventional polyamides prepared by polycondensation with polydispersities degrees between 1.2 and 1.9. Polyamides PA-*n*Mn exhibited high optical rotations as expected from the symmetry of the mannaramide unit whereas no optical activity was detected for either PA-*n*Xy or PA-*n*Ga, as expected.

The IR and NMR spectroscopies confirmed the structure of these polyamides. As L-arabinitol-, xylitol- and galactitol-based monomers are molecules without C_2 axis of symmetry, their polycondensation was expected to lead to aregic polyamides due to the non-regioselective addition of the monomers. In fact, the ^{13}C-NMR spectra of polyaldaramides made from such monomers showed three signals (one of them double) for the carbonyl groups, corresponding to the four stereochemical possibilities for the triads centred on the aldaric unit.

All the polyamides were soluble in the usual organic solvents including chloroform, but not soluble in water. Nevertheless, they were all found to be very hygroscopic as a consequence of the high number of methoxyl groups present in their repeating units. As expected, the water sorption diminished with the incremental increase of the methylene number in the polymethylene segment of the non-carbohydrate moiety. It was noticed that polyamides derived from xylitol were more hygroscopic than those derived from

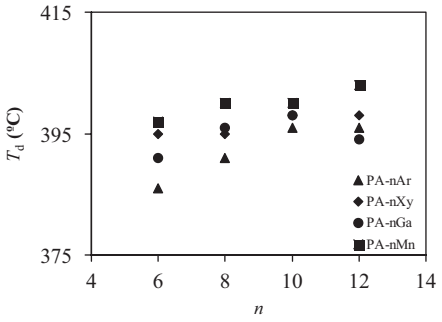

Figure 1. Variation of the decomposition temperature with the polymethylene length.

L-arabinitol, a result that is thought to be a consequence of the differences in crystallinity exhibited by these polyamides such as it will be discussed below.

Thermal properties. The thermal properties of polyaldaramides depend on both the configuration of the sugar unit and the length of the polymethylene segment contained in the diamine unit. The thermogravimetric analysis revealed that those polyamides are fairly stable to heat. Decomposition under an inert atmosphere appeared to happen in two well separated steps, the first taking place near 400°C and the second one at above 450°C. In Figure 1, the maximum rate temperature of the first step is plotted against the number of methylenes contained in the diamine for the four series. In general, the trend observed is that T_d increases with n although the influence of the constitution of the sugar was not clearly evidenced in these results.

The DSC analysis revealed that all these polyamides with the exception of PA-*n*Xy were semicrystalline. The heating DSC traces showed well defined melting peaks that were partially reproduced at reheating from the melt. In Figure 2(a) the melting temperature as a function of n is plotted for polyamides with *arabino*, *galacto* and *manno* configuration. The T_m values were within the range of 150 to 225°C with values decreasing steadily as the length of the diamine unit increased. ΔH_m was found to oscillate between 10 and 50 J g^{-1} with no apparent correlation with either the length of the alkylenediamine or the sugar configuration but with a clear correspondence with the size of the sugar unit. In Figure 3, the melting enthalpy of polyamides made from 1,6-hexamethylenediamine and *threo*, *arabino*, and *manno* aldaric acids are compared, illustrating how the crystallinity of these polyaldaramides decays almost linearly with the size of the sugar unit. In Figure 2(b), the T_g of polyaldaramides are plotted against n. The T_g span a range of around 50°C ranging approximately from 110 to 60°C with values decreasing as the values of n increased; the exceptionally low values found for polyamides with *xylo* configuration were most likely due to the absence of crystallinity.

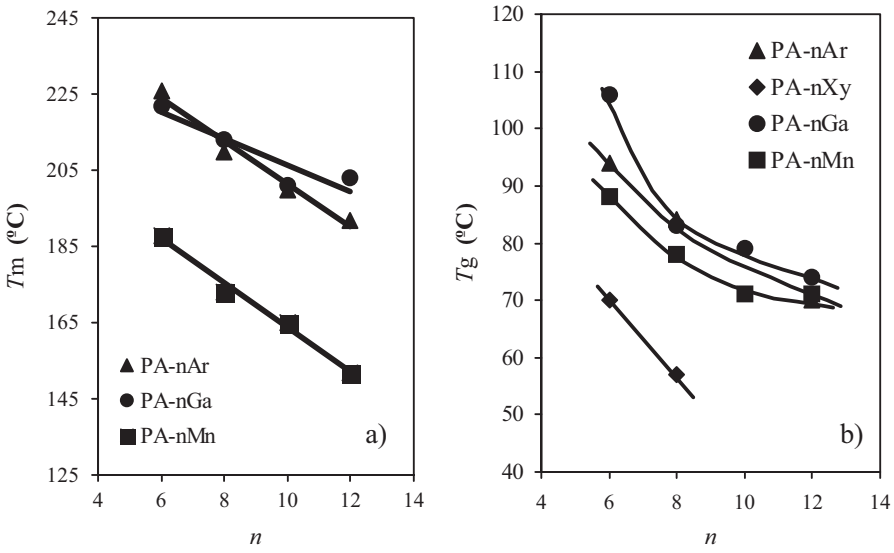

Figure 2. Variation of the melting and glass transition temperature with *n* for the different polyaldaramide series.

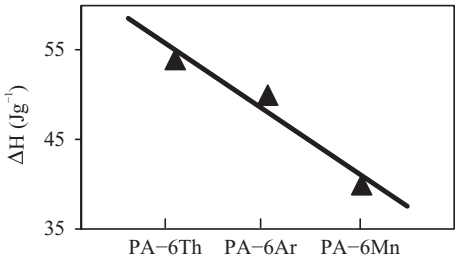

Figure 3. Compared melting enthalpies for polyaldaramides derived from aldaric acids of different size.

Crystal structure. The crystallinity of polyaldaramides firstly evidenced by DSC was faithfully reflected in their capacity for crystallizing under very different conditions. As shown in Figure 4 for some representative cases, they all afforded typical spherulitic textures in the crystallization from the melt. Although the crystallization rate and spherulitic morphologies depended largely on the chemical structure of the polyamide, it was really striking that they were able to crystallize for both symmetric and asymmetric configurations, as well as for any size of the sugar unit.

Furthermore, lamellar crystals and crystalline fibers could be prepared from all these polyaldaramides. For illustration, results attained with polyaldaramide PA-6Ar are shown in Figure 5. The lamellar crystals produced when this polyamide was left to crystallize isothermally from solution are shown in Figure 5(a) with the selected area electron diffraction pattern recorded from them included as an inset. Again the shapes and sizes of the crystals vary from one polyamide to another but the electron diffraction patterns suggested that they all crystallized following a similar model of chain packing. The wide-angle X-ray diffraction pattern recorded from a fiber of PA-6Ar that was stretched from the melt is shown in Figure 5(b). Although the pattern is not well oriented it displays discrete scattering characteristic of semicrystalline material.

The repeating unit of the polyaldaramide chain consists of two well differentiated moieties (Figure 6(a)). The aldaric acid moiety is a polymethyloxy group which is hydrophilic, bulky and protruding, and prone to adopt a skew conformation according to its configuration. The alkylenediamine moiety consists of a polymethylene segment which is hydrophobic, linear and flexible, and usually arranged in fully extended *all-trans* conformation. The irregular molecular constitution of these polyamides raises the question of how these chains can be packed efficiently to form the crystal lattice. Combination of experimental diffraction data with molecular modelling based on energy calculations afforded a detailed description of what can be the crystal structure of these polyaldaramides. The first studies carried out on PA-6Ar revealed that they crystallize, building the hydrogen-bonded sheets that are typical of nylons[32,33] with the chains adopting a skew conformation.[34] Figure 6(b) and 6(c) show a view normal to the sheet showing four hydrogen-bonded neighboring chains as well as an edge-on view of the four stacked sheets showing how chains that are bent are depicted. The sugar unit is placed at the kinks, and the polymethylene segment in *all-trans* conformation is tilted at a constant angle with respect to the *c*-axis of the structure. In this way the occupancy of the space is optimized and the polymethylene segments can approach each other as closer as it is required for crystallization.

PBT copolyesters

Synthesis and characterization. The synthesis of the copolyesters was carried out by the reaction of dimethyl terephthalate (DMT) and mixtures of 1,4-butanediol and

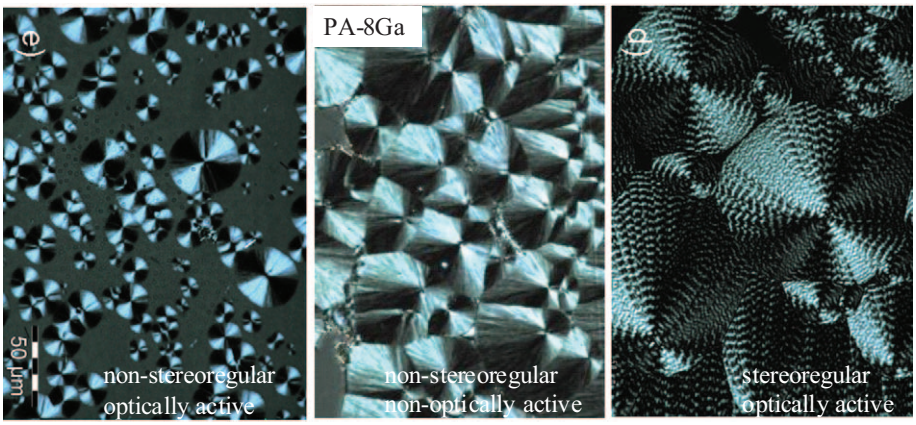

Figure 4. Spherulitic films of polyaldaramides crystallized from the melt.

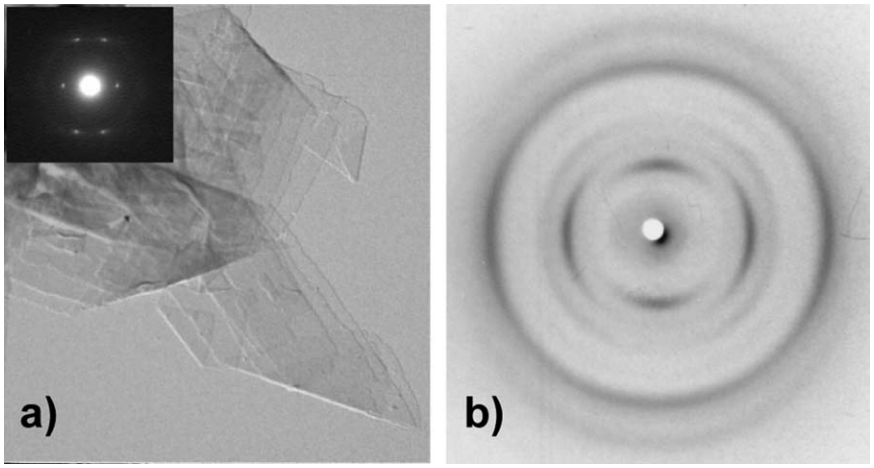

Figure 5. (a) Llamellar crystals of PA-6Ar obtained by isothermal crystallization from solution (Inset: electron diffraction pattern), and WAXS pattern of a fiber stretched from the melt (fiber axis is vertical).

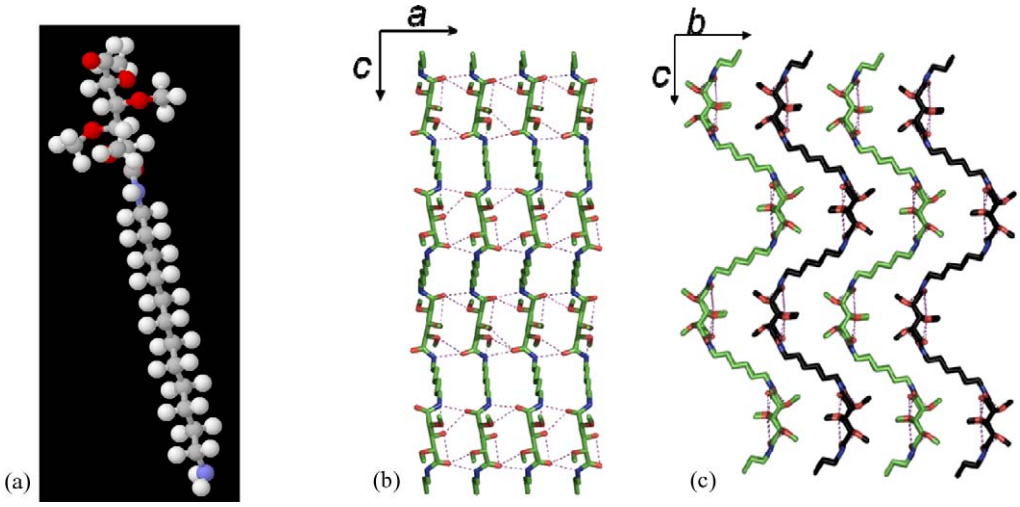

Figure 6. (a) Structure of the repeating unit of PA-6Ar. (b) View along the *b*-axis of the crystal structure showing a sheet with chains hydrogen bonded along the *a*-axis. (c) View of the *bc*-plane showing the stacking of the sheets along the *b*-axis.

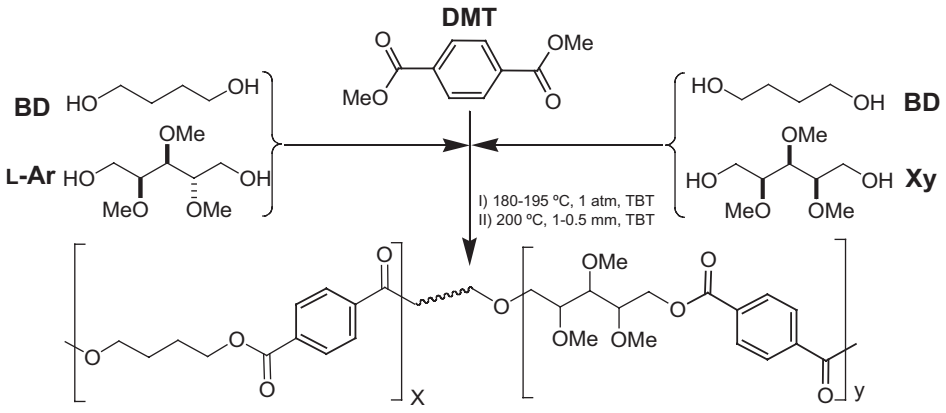

Scheme 6. Synthesis of PBT copolyesters.

Table 2. Composition, microstructure, molecular size and optical activity of polyesters and copolyesters.

Polyester	Composition[a] (X_B/X_P)		R^b (%)	$[\eta]^c$ (dL g^{-1})	$M_w{}^d$	PD^d	$[\alpha]_D{}^e$ (°)
PBT	100/0	100/0	–	1.07	45 700	2.3	–
co$PB_{90}Ar_{10}T$	90/10	88/12	0.93	0.40	31 000	1.9	~0
co$PB_{80}Ar_{20}T$	80/20	80/20	0.97	0.38	31 900	2.1	+1.6
co$PB_{70}Ar_{30}T$	70/30	67/33	1.03	0.44	42 100	2.0	+2.2
co$PB_{50}Ar_{50}T$	50/50	48/52	1.02	0.57	27 600	1.8	+5.9
PArT	0/100	0/100	–	0.29	21 000	1.5	+117
co$PB_{90}Xy_{10}T$	90/10	88/12	0.90	0.51	35 400	1.8	0
co$PB_{80}Xy_{20}T$	80/20	78/22	0.90	0.46	41 000	2.2	0
co$PB_{70}Xy_{30}T$	70/30	69/32	0.99	0.41	33 600	2.1	0
co$PB_{50}Xy_{50}T$	50/50	47/53	1.00	0.32	28 300	1.9	0
PXyT	0/100	0/100		0.28	19 000	1.6	0

[a]Composition of the feed and the resulting copolyester determined by ^{1}H-NMR. X_B and X_P = %-mole of 1,4-butanediol and pentitol, respectively.
[b]Composition randomness determined by ^{13}C-NMR.
[c]Intrinsic viscosity measured in dichloroacetic acid at 25°C.
[d]Weight-average molecular weights and polydispersity determined by GPC using chloroform as the mobile phase.
[e]Specific optical rotation measured at 25°C.

2,3,4-tri-*O*-methyl-L-arabinitol or 2,3,4-tri-*O*-methyl-xylitol in the selected proportions. For comparison purposes, the parent homopolyesters (PBT, PArT and PXyT) were prepared by the same procedure from their respective pure diols. The polycondensation reaction proceeded in the melt through two stages following the procedure commonly used on an industrial scale to prepare PET and PBT (Scheme 6).[35] In the first stage, transesterification of dimethyl terephthalate with the mixture of the two diols was accomplished with release of methanol. Polycondensation, leading to copolyesters containing arabinitol (*co*PB_xAr_yT) or xylitol units (*co*PB_xXy_yT) or to homopolyesters, took place in the second stage under vacuum at higher temperatures to facilitate the removal of the exceeding diol. Copolyesters were prepared from feed molar ratios of BD: alditol ranging from 90: 10 to 50: 50.

The chemical constitution and composition of the resulting polycondensates were ascertained by ^{1}H-NMR and their molecular weights were estimated by GPC and viscosimetry. Data provided by these analyses are given in Table 2, where it can be seen that the copolyesters had compositions essentially similar to those of their respective feeds. The weight-average molecular weights of the polymers were found to be within the 20 000 to 45 000 range, corresponding to intrinsic viscosities between 0.3 and 1.1 dL g^{-1}. As expected from the configuration of the alditols used, polyesters and copolyesters made from optically active Ar displayed weak optical rotations, while no activity at all was observed for those containing Xy units.

The microstructure of copolyesters was determined by ^{13}C-NMR analysis. These spectra showed complex signals for the aromatic carbons of the terephthalic units, indicating that these units were sensitive to sequence effects. As shown in Figure 7 for the case of *co*PB_xXy_yT copolyesters, the resonance of the nonprotonated aromatic carbon appeared as four signals in the 133.3–134.3 ppm chemical shift interval, corresponding to the three types of dyads (BTXy or XyTB, BTB, and XyTXy that were possible

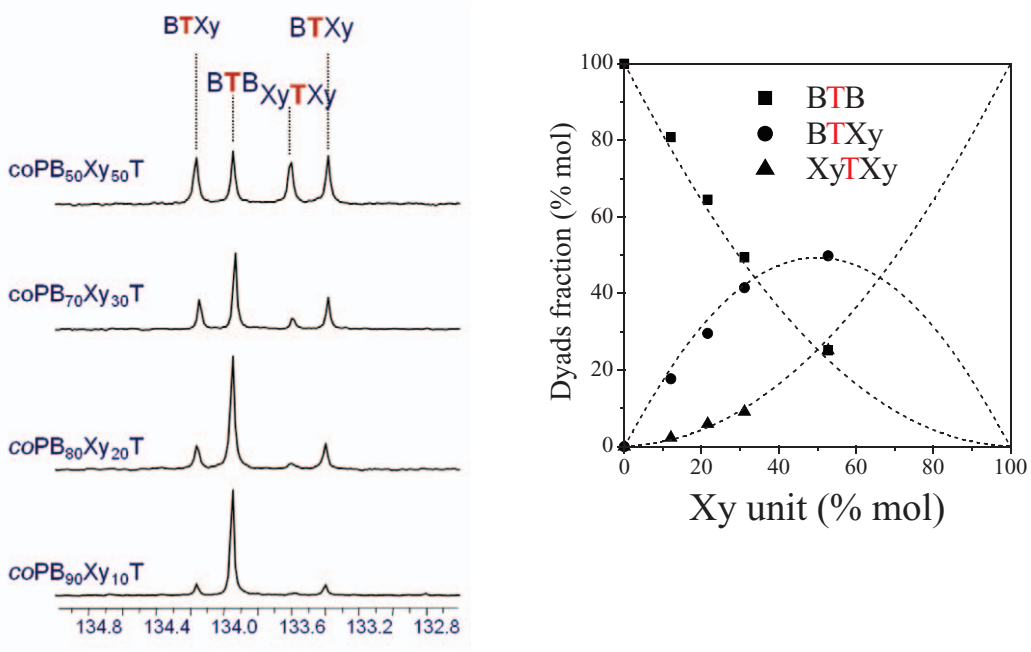

Figure 7. Left: Signals arising from the T-centred dyads of *co*PB$_x$Xy$_y$T. Right: Dyad contents against copolyester composition.

Table 3. Thermal properties of polyesters and copolyesters.

	DSC			TGA	
	T_m (°C)	ΔH_m (J g^{-1})	T_g (°C)	T_d[a] (°C)	ΔW[b] (%)
PBT	221	67.1	30	407	8
coPB$_{90}$Ar$_{10}$T	211	46.1	35	405	9
coPB$_{80}$Ar$_{20}$T	185	28.4	36	405	8
coPB$_{70}$Ar$_{30}$T	151	11.4	43	357/**402**	5
coPB$_{50}$Ar$_{50}$T	–	–	50	370/**400**	3
PArT	91	27	60	374	0
coPB$_{90}$Xy$_{10}$T	206	56.0	34	409	8
coPB$_{80}$Xy$_{20}$T	185	38.0	33	407	4
coPB$_{70}$Xy$_{30}$T	157	16.3	35	351/**407**	4
coPB$_{50}$Xy$_{50}$T	–	–	44	365/**399**	3
PXyT	–	–	50	364	0

[a]Temperature of maximum degradation rate.
[b]Remaining weight at the end of the decomposition process.

along the copolyester chain. The plot of the content in each type of dyad as a function of the copolyester composition revealed that the microstructure of the copolyester was almost statistical with randomness quite near unity in all cases.

Thermal properties and crystal structure. The thermal behavior of copolyesters was comparatively studied by DSC and TGA and the thermal parameters resulting from these analyses are given in Table 3. Regarding thermal stability, it was observed that although the insertion of the methylated pentitols promoted a moderate decrease in the resistance to heat, all the copolymers remained essentially unaltered up to 300°C.

The DSC analysis showed that copolymerization introduced significant changes in both melting and glass transition temperatures of the parent polymer PBT. Glass temperature was found to span between 30 and 60°C and to increase almost steadily with the content in alditol units, which is fully consistent with the high values observed for the PArT and PXyT homopolyesters. On the other side, well-defined melting peaks, indicative of the presence of a crystalline phase were observed for copolyesters containing up to 30% of pentitol units. Although the crystallinity decreased in both series with the content in alditol, and PXyT was amorphous, the homopolyester PArT was crystalline in spite of being non-stereoregular. It is clear that the crystallinity of polyesters was

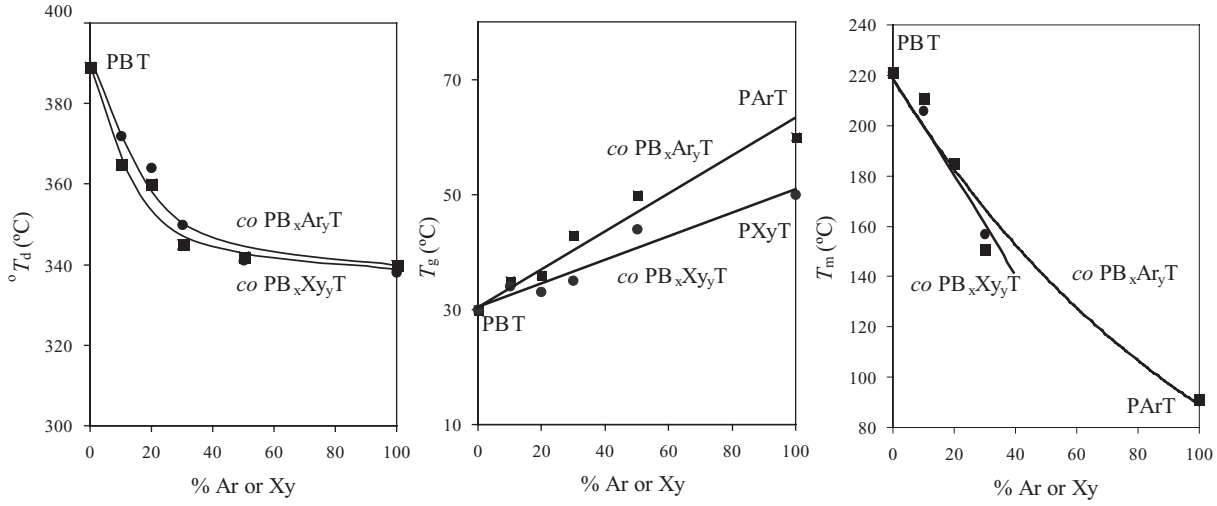

Figure 8. Variation of decomposition (T_d), melting (T_m), and glass transition (T_g) temperatures of polyesters with the content in alditol units.

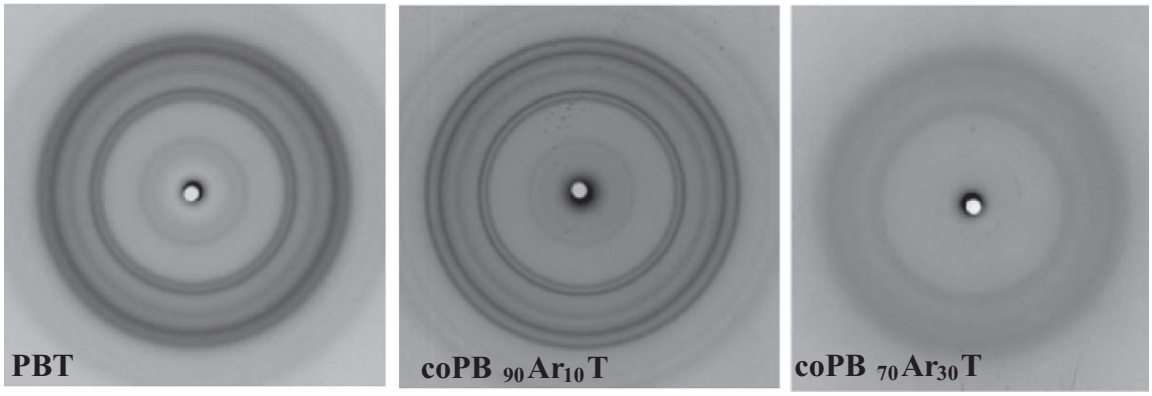

Figure 9. Powder WAXS patterns of PBT and its copolyesters containing arabinitol units.

dependent on the configuration of the sugar residue and that dilution of the sugar units in the copolyesters suppressed the configurational effects operating in the homopolymers. The trend observed in the decomposition, glass transition and melting temperatures with the variation in the composition of the copolyester is graphically depicted in the plots of Figure 8.

The powder X-ray diffraction analysis corroborated the DSC data. Representative WAXS powder patterns are compared in Figure 9. These patterns clearly show how crystallinity decreased with the content in alditol, so the pattern recorded from the copolyester containing 30% of arabinitol was very weak and diffuse. Nevertheless, it is worth noticing that the same basic pattern regarding both spacing and intensities was shared by all the copolymers revealing that the triclinic crystal structure of PBT was retained in the copolyesters.[36] Whereas it is thought that a length of at least 15–20 BT repeating-units is the minimum required for crystallization,[37] other observations have revealed that

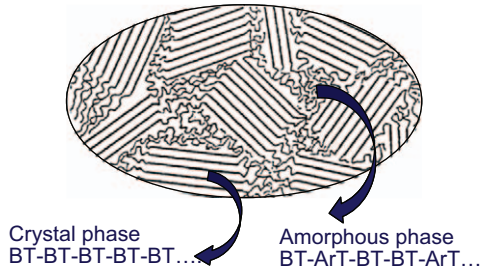

Figure 10. Distribution of copolyester sequences in the biphasic semicrystalline state.

certain PBT copolymers are able to crystallize for chain segments consisting of only two to five repeating units.[38] A question immediately arises with respect to the location of the pentitol units in the biphasic semicrystalline state. Although this point has not been studied in detail it does make sense to interpret the behavior that the crystal phase of the copolyesters was made

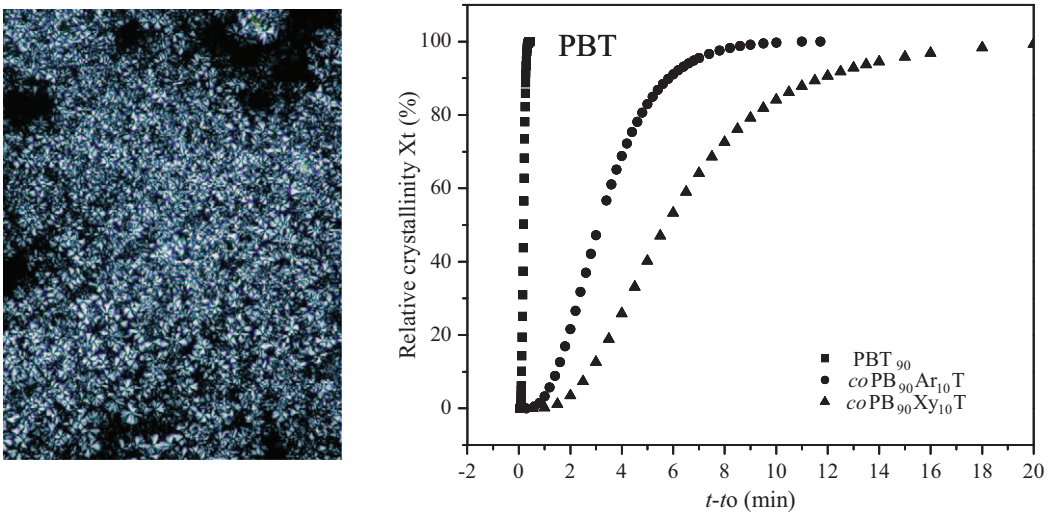

Figure 11. Spherutitic film of *co*$PB_{90}Ar_{10}$ T crystallized from the melt at 190°C (left) and compared crystallization isotherms of PBT and the indicated copolyesters (right).

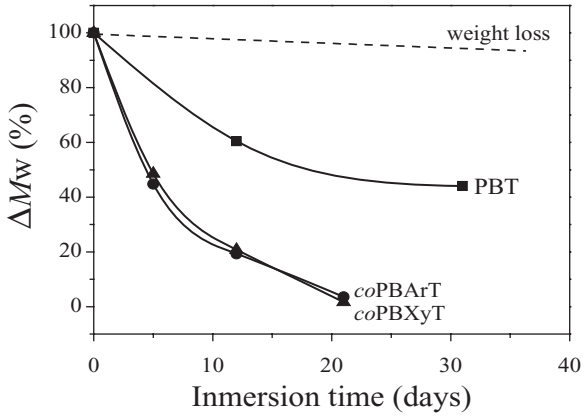

Figure 12. Evolution of sample and molecular weights of PBT and its 50:50 copolyesters with incubation time.

exclusively of alkylene terephthalate sequences whereas the sequences containing alditol units were rejected by the amorphous phase (Figure 10).

One of the main factors determining the wide applicability of PBT in the manufacture of injection-made pieces was its high crystallizability. This results from the high crystallization rate and high degree of crystallinity that PBT was able to attain when it solidified upon cooling from the melt. To evaluate the influence of the insertion of alditol units on the crystallizability of PBT, the isothermal crystallization of the homopolyester and copolyesters was comparatively studied and the kinetics parameter estimated on the basis of the Avrami approach. Figure 11 shows a film of the copolyester *co*$PB_{90}Ar_{10}T$ crystallized from the melt at 190°C and the isothermal traces showing the advance of crystallinity with time for the crystallization of the copolyesters containing 10% of arabinitol oxylitol. The half-crystallization times of 0.09, 1.50 and 5.15 min were estimated for these three polymers, respectively.

It was concluded that the incorporation of alditol units depressed the crystallizability of PBT by decreasing both the crystallinity and the crystallization rate, and that these effects were more pronounced in the xylitol copolyesters.

Hydrolysis. The incorporation of sugar units in PBT enhances its hydrophilicity and therefore an increase of its sensitivity to hydrolysis should be expected. The hydrolysis of some copolyesters was examined and compared with that of PBT to evaluate their influence. The evolution of the sample weight and molecular weight of the copolyesters 50/50 of arabinitol and xylitol with incubation time in the aqueous buffer both at pH 10 at 80°C compared with PBT is shown in Figure 12.

Whereas no significant changes in weight loss was observed, it was found that the molecular weight decreased largely at a rate that increased with the incorporation of alditols units and that this effect was similar for arabinitol and xylitol.

It has been reported[39] that ^{1}H-NMR spectra of PET copolyesters $PE_{50}A_{50}T$ and $PE_{50}Xy_{50}T$ subjected to hydrodegradation for 90 days displayed significant changes with respect to those of the original co-polyesters (Figure 13). The changes mainly affected the sugar proton signals, revealing that the degradation process took place essentially by cleavage of the ester linkages associated with the alditol units. Furthermore, the analysis by scanning electron microscopy of an incubated film of the homopolyesters PArT revealed how hydrolysis takes place at the morphological level. As shown in Figure 14, the pristine smooth film was severely eroded so the thickness was reduced to about half of the initial value. A plentiful amount of material made of nonsoluble fragments generated by hydrolysis was deposited on the surface. As this material was not released to the medium, the sample weight was expected to remain apparently unchanged.

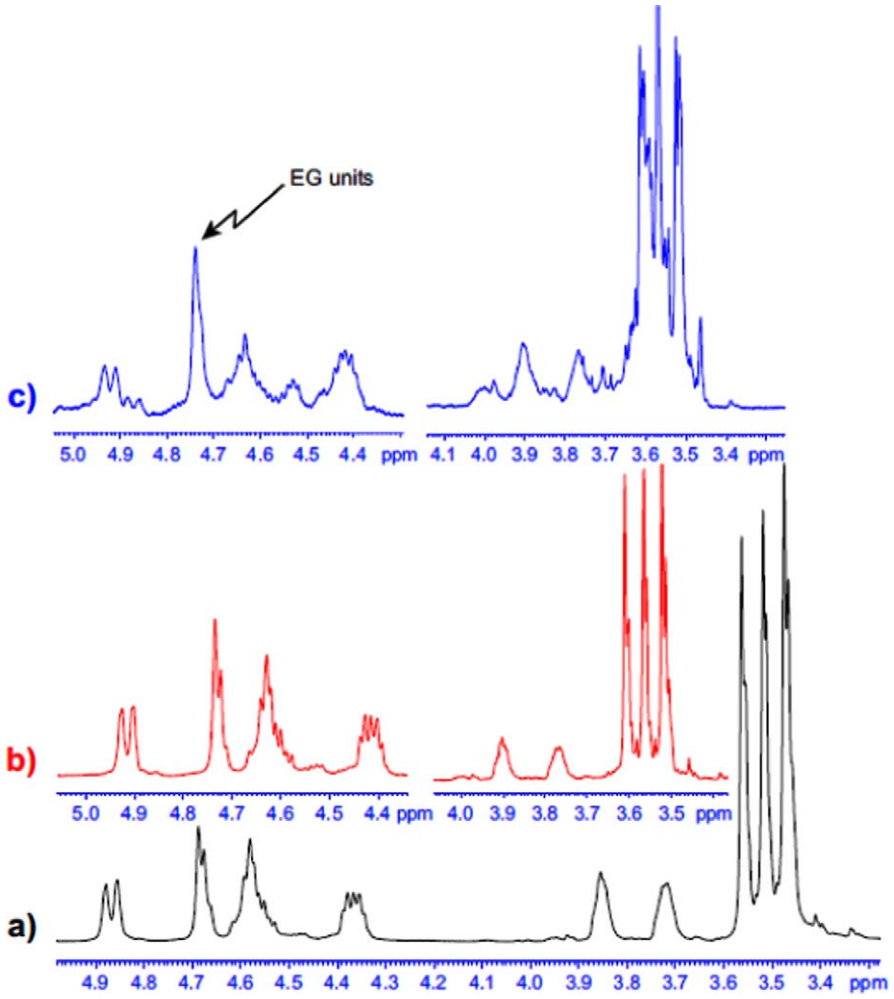

Figure 13. ^{1}H-NMR spectra of $PE_{50}Ar_{50}$ T copolyester upon incubation in buffer pH 4.0.

The information provided by GPC and NMR spectroscopy of aromatic copolyesters containing alditols units allowed a rough scheme describing the mechanism that operates in the hydrolytic degradation of PBT copolyesters to be outlined (Scheme 7). Hydrolysis would take place preferentially on the aldilene terephthalate ester bond. Soluble

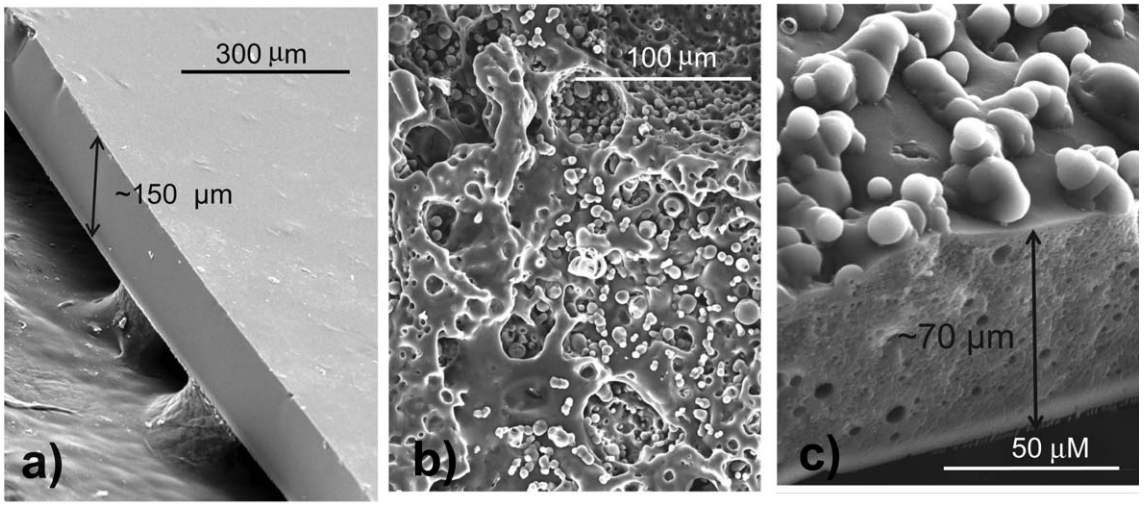

Figure 14. SEM micrographs of PArT before (a) and after (b, c) incubation at pH 4.0 for 60 days; (b) surface view; (c) edge-view.

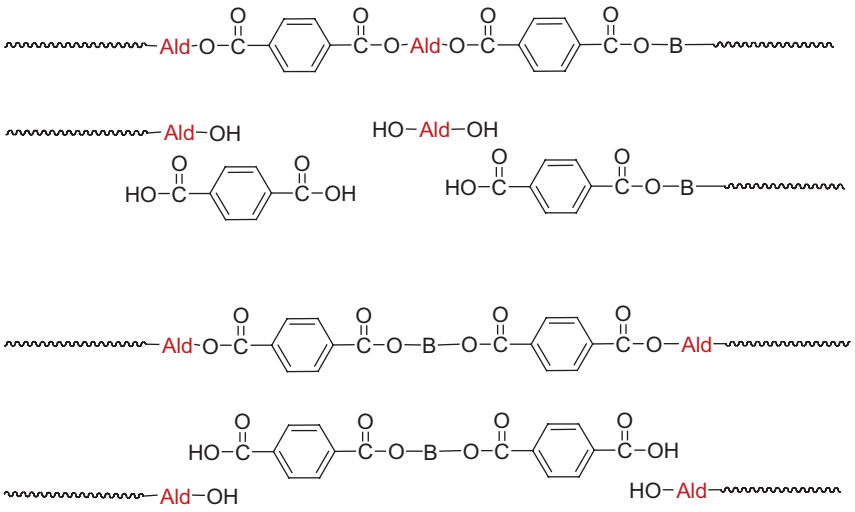

Scheme 7. Proposed scheme of the hydrolytic degradation of alditol containing PBT copolyesters. Ald: alditol unit; B: butylene unit

alditol will therefore be generated from complete hydrolysis of the aldilene terephthalate units. Sequences consisting of aldilene–aldilene dyads will therefore generate terephthalic acid. Butylene terephthalate units will remain relatively unaltered and in the case that they are jointed to two aldilene units, then non-water-soluble butylene diterephthalate will be produced. More or less longer segments will be generated depending on the composition and sequence distribution and they will end in alditol or terephthalic groups in equal amounts. These fragments are supposed to be non-water-soluble and therefore remain attached to the sample.

Concluding remarks

The preparation of aregic linear polyamides of the AABB-type using fully O-mehylated aldaric acids derived from naturally occurring aldopentoses l-arabinose and d-xylose and aldohexoses D-galactose and D-mannose, is feasible by polycondensation with alkanediamines. The properties of these carbohydrate-based polyamides depend on their constitution, and in some extent, on the configuration of the carbohydrate-based moiety. All the polyamides are soluble in the usual organic solvents and very hygroscopic but remain to be non-soluble in water. The incorporation of sugar units increase the T_g of polyaldaramides with regards to their nylon homologues and increases slightly their thermal stability. All the polyamides except poly(xylaramide)s are semicrystalline and able to crystallize from the melt. T_m and also T_g decrease within each series with the increasing length of the diamine segment. The crystal structure of polyaldaramides follows the pattern of nylons with chains hydrogen-bonded in sheets but with chains in a bended conformation to make possible the accommodation of the sugar units in the crystal space.

Preparation of PBT copolyesters containing up to 50% of trimethoxy pentitols derived from naturally occurring L-arabinose and D-xylose is feasible by polycondensation in the melt. The copolyesters have acceptable molecular weights and a random microstructure. They are semicrystalline up to contents of 30% pentitol and retain the crystal structure of PBT. The melting temperature of PBT is considerably depressed by the presence of the pentitol units, but its glass transition temperature increases and the thermal stability is scarcely affected. The crystallizability is also diminished by copolymerization, although the copolymers with 10 and 20% of pentitol units continue to be readily crystallizable from the melt. The copolymers are much more sensitive to hydrolysis than PBT, this effect being scarcely depending on the configuration of the sugar unit.

Acknowledgments

This work is presented as a representative piece of a combined long-term project carried out by the Universidad Politècnica de Catalunya and the University of Sevilla, which is addressed to the research of new sustainable polycondensates made from natural carbohydrates. Financial support for this project was afforded by MICINN (Ministerio de Ciencia e Innovación) with successive grants and currently supported by grant MAT2009-14053-C02.

References

1. Wool R and Sun S. *Biobased polymers and composites*. Amsterdam: Academic Press, 2005.
2. Wang Q, Dordick JS and Linhardt RJ. Synthesis and application of carbohydrate-containing polymers. *Chem Mater* 2002; **14**: 3232–3244.
3. Galbis JA and García-Martín MG. In Sugars as monomers. Belgacem MN and Gandini A (eds) *Monomers, polymers and*

composites from renewable resources. Oxford, UK: Elselvier, 2008, pp. 89–114.
4. Bou J, Rodríguez-Galán A and Muñoz-Guerra S. Biodegradable optically active polyamides. In: *The polymeric materials encyclopedia*. Boca Raton, FL: CRC Press, 1996, **vol. 1**, p. 561.
5. Rodríguez Galán A, Bou JJ and Muñoz-Guerra S. Stereoregular polyamides derived from di-*O*-methylene-L-tartaric acid and aliphatic diamines. *J Polym Sci, Polym Chem* 1992; **30**: 713–721.
6. Bou JJ, Rodríguez Galán A and Muñoz-Guerra S. Optically active polyamides derived from L-tartaric acid. *Macromolecules* 1993; **26**: 5664–5670.
7. Bueno M, Galbis JA, García-Martín MG, de Paz MV, Zamora F and Muñoz-Guerra S. Synthesis of stereoregular polygluconamides from D-glucose and D-glucosamine. *J Polym Sci, Polym Chem* 1995; **33**: 299–305.
8. Regaño C, Mtz de Ilarduya A, Iribarren I, Rodríguez-Galán A, Galbis JA and Muñoz-Guerra S. Stereocopolyamides derived from 2,3-di-*O*-methyl-D and L-tartaric acids and hexamethylene-diamine. *Macromolecules* 1996; **29**: 8404–8412.
9. Alla A, Rodríguez-Galán A, Mtz de Ilarduya A and Muñoz-Guerra S. Degradable poly(ester amide)s based on L-tartaric acid. *Polymer* 1997; **38**: 4935–4944.
10. Zamora F, Bueno M, Molina I, Iribarren I, Muñoz-Guerra S and Galbis JA. Stereoregular copolyamides derived from D-xylose and L-arabinose. *Macromolecules* 2000; **33**: 2030–2038.
11. Esquivel D, Bou JJ and Muñoz-Guerra S. Synthesis, characterization and degradability of polyamides derived from tartaric acid and diaminoethers. *Polymer* 2003; **44**: 6169–6177.
12. Majó MA, Alla A, Bou JJ, Herranz C and Muñoz-Guerra S. Synthesis and characterization of polyamides obtained from tartaric acid and L-lysine. *Eur Polym J* 2004; **40**: 2699–2708.
13. Kint DPR, Wigström E, Mtz de Ilarduya A, Alla A and Muñoz-Guerra S. Poly(ethylene terephthalate) copolyesters derived from (2*S*,3*S*)2,3-dimethoxy-1,4-butanediol. *J Polym Sci, Polym Chem* 2001; **39**: 3250–3262.
14. Zamora F, Hakkou K, Alla A, Rivas M, Roffé I, Mancera M and Muñoz-Guerra S. Aromatic polyesters from naturally occurring monosaccharides: Poly(ethylene terephthalate) and poly(ethylene isophthalate) analogs derived from D-mannitol and galactitol. *J Polym Sci, Polym Chem* 2005; **43**: 4570–4574.
15. Zamora F, Hakkou K, Alla A, Espartero JL, Muñoz-Guerra S and Galbis JA. Aromatic homo- and copolyesters from naturally occurring monosaccharides: PET and PEI analogs derived from L-arabinitol and xylitol. *J Polym Sci, Polym Chem* 2005; **43**: 6394–6410.
16. Zamora F, Hakkou K, Alla A, Marín-Bernabé A, de Paz MV and Mtz de Ilarduya A Muñoz-Guerra S. Polyesters analogous to PET and PBT based on *O*-benzyl ethers of xylitol and L-arabinitol. *J Polym Sci, Polym Chem* 2008; **46**: 5167–5179.
17. Zamora F, Hakkou K, Alla A, Rivas M, Mtz de Ilarduya A, Muñoz-Guerra S and Galbis JA. Butylene copolyesters based on aldaric and terephthalic acids. Synthesis and characterization. *J Polym Sci, Polym Chem* 2009; **47**: 1168–1177.
18. Alla A, Rodríguez-Galán A, Mtz de Ilarduya A and Muñoz-Guerra S. Degradable poly(ester amide)s based on L-tartaric acid. *Polymer* 1997; **38**: 4935–4944.
19. Villuendas I, lribarren I and Muñoz-Guerra S. Poly(ester amide)s derived from L-tartaric acid and amino alcohols I. Regic polymers. *Macromolecules* 1999; **32**: 8015–8023.
20. Villuendas I, Molina I, Regaño C and Muñoz-Guerra S. Hydrolytic degradation of poly(ester amide)s made from tartaric and succinic acids: influence of the chemical structure and microstructure on degradation rate. *Macromolecules* 1999; **32**: 8033–8040.
21. Regaño C, Mtz de Ilarduya A, Iribarren JI and Muñoz-Guerra S. Poly(ester amide)s derived from L-tartaric and amino alcohols II. Aregic polymers. *J Polym Sci, Polym Chem* 2000; **38**: 2687–2696.
22. Alla A, Rodríguez Galán A and Muñoz-Guerra S. Hydrolytic and enzymatic degradation of copoly(ester amide)s based on L-tartaric and succinic acids. *Polymer* 2000; **41**: 6995–6702.
23. Pérez-Rodríguez A, Alla A, Fernández-Santín JM and Muñoz-Guerra S. Poly(ester amide)s derived from tartaric and succinic acids: Changes in structure and properties upon hydrolytic degradation. *J Appl Polym Sci* 2000; **78**: 486–494.
24. Villuendas I, Bou JJ, Rodríguez Galán A and Muñoz-Guerra S. Alternating copoly(ester amide)s derived from amino alcohols and L-tartaric and succinic acids. *Macromol Chem Phys* 2001; **202**: 236–244.
25. Regaño C, Marín R, Alla A, Iribarren JI and Muñoz-Guerra S. Crystallization and crystal structure of poly(ester amide)s derived from L-tartaric acid. *J Polym Sci, Polym Phys* 2006; **45**: 116–125.
26. García-Martín MG, Pérez RR, Hernández EB, and Espartero JL, Muñoz-Guerra S and Galbis JA. Carbohydrate-based polycarbonates Synthesis, structure, and biodegradation studies. *Macromolecules* 2005; **38**: 8664–8670.
27. Mancera M, Zamora F, Roffe I, Bermúdez M, Alla A, and Muñoz-Guerra S and Galbis JA. Synthesis and properties of poly(D-mannaramide)s and poly(galactaramide)s, *Macromolecules* 2004; **37**: 2779–2783.
28. García-Martin MG, Hernández EB, Pérez E, Alla A , Muñoz-Guerra S and Galbis JA. Synthesis and characterization of linear polyamides derived from l-arabinitol and xylitol. *Macromolecules* 2004; **37**: 5550–5556.
29. Alla A, Hakkou K, Zamora F, Mtz de Ilarduya A, Galbis JA and Muñoz-Guerra S. Poly(butylene terephthalate) copolyesters derived from l-arabinitol and xylitol. *Macromolecules* 2006; **39**: 1410–1416.
30. García-Martín MG, Ruíz Pérez R, Benito Hernández E and Galbis JA. Synthesis of L-arabinitol and xylitol monomers for the preparation of polyamides. Preparation of an L-arabinitol-based polyamide. *Carbohydr Res* 2001; **333**: 95–103.
31. Mancera M, Roffé I, Rivas M and Galbis JA. New derivatives of D-mannaric and galactaric acids. Synthesis of a new stereoregular nylon 66 analogue from carbohydrate-based monomers having the D-manno configuration. *Carbohydr Res* 2003; **338**: 1115–1119.

32. Bunn CW and Garner EV. The crystal structures of two polyamides ('nylons'). *Proc Roy Soc* 1947; **A 189**: 39–68.
33. Holmes DR, Bunn CW and Smith DJ. The crystal structure of polycaproamide: nylon 6. *J Polym Sci* 1955; **7**: 159–177.
34. Muñoz-Guerra S, Fernández C, Benito E, Marín R, García-Martín MG, Bermúdez M and Galbis JA. Crystalline structure and crystallization of stereoisomeric polyamides derived from arabinaric acid. *Polymer* 2009; **50**: 2038–2057.
35. Sheirs J and Long TE. *Modern polyesters*. Wiley Series in Polymer Science. West Sussex, UK: Wiley, 2003.
36. Hall IH and Pass MG. Chain Conformation of Poly(Tetramethylene terephthalate) and its change with strain. *Polymers* 1976; **17:** 807–816.
37. Marchese P, Celli A and Fiorini MJ. Relationships between the molecular architecture, crystallization capacity, and miscibility in poly(butylene terephthalate) /polycarbonate blends: A comparison with poly(ethylene terephthalate)/polycarbonate blends. *J Polym Sci, Polym Phys* 2004; **42**: 2821–2832.
38. Kuwabara K, Gan ZH, Nakamura T, Abe H and Doi Y. Crystalline/amorphous phase structure and molecular mobility of biodegradable poly(butylene adipate-co-butylene terephthalate) and related polyesters, *Biomacromolecules* 2002; **3**: 390.
39. Zamora F, Hakkou K, Muñoz-Guerra S and Galbis JA. Hydrolytic degradation of carbohydrate-based aromatic homo- and co-polyesters analogous to PET and PEI. *Polym Degrad Stab* 2006; **91**: 2654–2659.